Numerical and Experimental Dynamic Analysis of 3D-Printed Pierced Vault

Numerical and Experimental Dynamic Analysis of 3D-Printed Pierced Vault*

Raffaele Cucuzza[0000−0002−9344−6006], Amedeo D. B. Manuello Bertetto[0000−0003−1474−0176], Marco Domaneschi[0000−0002−6077−8338], Raffaele Tarantini[0000−0002−5769−829X], Alessandro Cardoni[0000−0002−9972−2702], and Gian paolo Cimellaro[0000−0001−6474−3493]

Department of Structural, Geotechnical and Building Engineering. Politecnico di Torino, Corso Duca degli Abruzzi, 24 - 10129. Torino, Italy
raffaele.cucuzza@polito.it

Abstract. In the present paper, a form-finding of shallow grid shells was introduced based on the multi-body rope approach (MRA) for the definitions of vaults with optimized shapes and different hole percentages. In order to obtain experimental validation, a physical model was reproduced at the laboratory scale performing ad hoc measurements to compare the observed respect to the simulated behaviour. A 3D printing procedure based on the Fuse Deposition Modeling (FDM) technique in polylactide (PLA) material was used to realize formworks of the cement-based blocks of the scaled prototype. Several static and dynamic load configurations are investigated, collecting the parameters into a sensitivity analysis, which mainly affects the structural behaviour. To compare the natural frequency obtained by experimental tests with those evaluated with a numerical model, an impulse test has been performed. Results show that an improvement in the modelling strategies adopted for the numerical model is necessary for the identification of the real structural dynamic response of the vault.

Keywords: Multi-body Rope Approach · Shape Optimization · Vaults · Dynamic Behaviour of Shells · Fuse Deposition Modeling · Experimental Dynamic Evaluation.

1 Introduction

Several authors have developed novel applications for masonry structures over the past 20 years, integrating them into real-world architectural and engineering settings while using cutting-edge realizations and design methodologies (e.g. [1], [2]). Due to the pressing environmental issue, innovative structural solutions that can balance structural efficiency and sustainability requirements are needed. Additionally, because of the development of optimization techniques (e.g. [3], [4], [5], [6], [7] and [8]), generative design and parametric analysis ([9]),

* Supported by ADDOPTML Project, MSCA RISE 2020 Marie Skodowska Curie Research and Innovation Staff Exchange

masonry buildings are once again in the forefront of the architectural and technical world. The idea of structural design has been transformed by computer-based design and modelling processes that produce comprehensive methods for shape, material, and structures (e.g. [10], [11]). In this area, the development of non-conventional and free-form structures was greatly aided by innovative shape-finding approaches based on automated tools and digital fabrication processes. Visual representation is necessary to give creative structural and architectural solutions (e.g. [12]) and real-time reactions (e.g. [1]) of buildings information have assumed a crucial role. Due to the durability of this specific structural topology and the high cost of raw materials for their chip extraction operation, there is a growing interest in studying ancient masonry vaults that have been built all over the world.

The issue of doubly-curved shells has emerged in recent decades and either compression-only vault design or curved surface design that takes into consideration the funicular's permanent structure is extensively treated by most publications (e.g. [1], [13]). Additionally, early research in this area focused on hanging models and graphic statics to study dome-shaped buildings. Antoni Gaud was the first to use a hanging scaled model in the design of the Crypt of Colonia Güell at the turn of the 20th century, as was extensively covered in [1].

Recently, new optimization approaches have been created and applied to grid shells in an effort to determine the ideal topology, form, and size for the members that make it up (e.g. [14]). By selecting a number of variables and placing them under a number of restrictions, optimization is the process of determining the least or maximum value of a function.

Among these, the most promising form-finding methodologies, that seek to identify the optimal form and topological configuration, are the well-liked technique force density method [15] and the dynamic relaxation (DR) [16].

In the present paper, the shape of the vault model is principally obtained by a form-finding method (MRA technique) fine-tuned by one of the authors [13]. The uniqueness of this approach consists of its adaptation to situations involving free forms with standardised constituent parts. In fact, one of the goals of this study is to provide an assessment that takes into account the best option among the many patterns of the perforated configurations (disposition of the holes) in addition to the usefulness of the form-finding approach used.

The analysis of the effects of a few selected parameters, including the lowering degree (defined as the ratio between the maximum span D and h, defined as the height of the vault), the slack coefficient of the original hanging net, and the hole percentage (HP) of the covering surface, yields the final geometric configuration of the vault. The final shape and the pierced pattern were analysed by the MidasGen©software under static and seismic load pattern configuration once constraint conditions were fixed.

The manufacturing process, [17], was adopted with the aim of achieving a scaled prototype of the selected vault typology. Moreover, a geometric survey was necessary to obtain, with a certain level of confidence, the input geometric data for numerical analysis as *Mechanical Autocad*©3d Model of the scaled-prototype.

Finally, to compare the natural frequency obtained by experimental tests with those evaluated with a numerical model, an impulse test has been performed. Results show that an improvement in the modelling strategies adopted for the numerical model is necessary for the identification of the real structural dynamic response of the vault.

2 Case Study: Vault Scaled-Prototype

A scaled-prototype of the reverse suspended net was created in order to evaluate the form-finding process utilising the MRA technique and to perform the test. The model measures 30 cm tall in total. In order to scale the previously described measurements to have a side equal to 1 m, a scaling method was performed using a scaling factor of 0.0625 (1/16). The scaled-prototype vault was 469 mm tall after this process, with a transverse section of 18.75 mm and a slenderness of 80. The appropriate bricks that made up the grid's rods were broken up into sections across the vault. For the final assembling step, a sequential numbering of the bricks was established, with each formwork corresponding to a particular brick. After this analysing the overall behaviour of the structure under a well-specified load pattern represents a crucial step for the success of the procedure. The vault's form was divided into numerous dowels using fast prototyping toolkits. Since the bricks must be produced in mortar cement, a moulding architecture must be developed. The correctness of the formwork geometry must be guaranteed due to the tiny scale of the model. The geometry of each formwork was entered into Rhinoceros with this goal in mind using the parametric CAD program Grasshopper. Therefore, after obtaining the geometric characteristics of the moulds, they were sent as input data to a 3D Bio-printer using the Fuse Deposition Modeling (FDM) process and entirely eco-friendly PLA material. The following are the most important settings made for 3D printing: 1.75 mm filament diameter, 0.2 mm layer height, and 0.1 fill density of 30%. The printing temperature was 215 C°, and the print speed ranged from 80 to 150 mm/s. It is noted that the four basic pieces were produced using the FDM method for the purpose of simplicity. Every brick used in the shuttering was cast, and the cement mortar used had a water-to-cement ratio of 0.4.

3 Experimental Set-up and Dynamic Test

Dynamic testing of structures can provide valuable information on the performance of structures (e.g. [18], [19] and [20]). Modal parameters (e.g. natural frequencies, mode shapes, and damping) can be determined from the measured dynamic response that is caused by ambient or forced vibration. The performance of the structure can then be characterised using these identified parameters, and analytical models can subsequently be validated [21]. This section outlines the dynamic tests performed on a shallow grid shell at the MASTRLAB laboratory (Politecnico di Torino, Italy), as well as the information regarding the instrumentation employed in the data acquisition processes.

3.1 Instrumentation

The instrumentation employed during the dynamic tests included a laptop provided with LabVIEW software, a data acquisition device, and No.2 accelerometers, which allowed us to identify the structure's acceleration response. The TE Connectivity model 4030 triaxial MEMS DC accelerometers (see Fig. 1) were used. They have a $2g$ dynamic range with a nominal $0 - 200$Hz bandwidth. The sensors' characteristics are shown in Table 2.

Fig. 1. Model 4030 triaxial MEMS DC accelerometer.

Table 1. Accelerometer's specifications.

Range (g)	±2g
Sensitivity (mV/g)	1000
Frequency response (Hz)	0-200
Excitation Voltage (Vdc)	5-30
Cable	6 x 0.14mm Conductors PVC Insulated, Braided Shield, PVC Jacket
Weight (grams)	50 (cable not included)

The data acquisition system consisted of a National Instruments (NI) USB-6211. It is a No.16 analogue input (16-Bit, 250 kS/s), No.2 analogue output (250 kS/s), No.4 digital input, No.4 digital output USB Multifunction I/O Device (see Fig. 2) which provides the accelerometers connection. An ad hoc LabVIEW software was developed to record the data.

3.2 Set-up

As shown in Fig. 3, the structure was located at the floor level, inside the MASTRLAB laboratory. The plywood base was loaded with steel elements to increase its mass and avoid any unwanted movement. To analyse the response of the structure, a triaxial MEMS accelerometer was installed on the top of the grid shell. A similar sensor was rigidly fixed to one of the four supports, close to the structure's impost (see Fig. 4). Both sensors were installed according to

Fig. 2. National Instruments USB-6211.

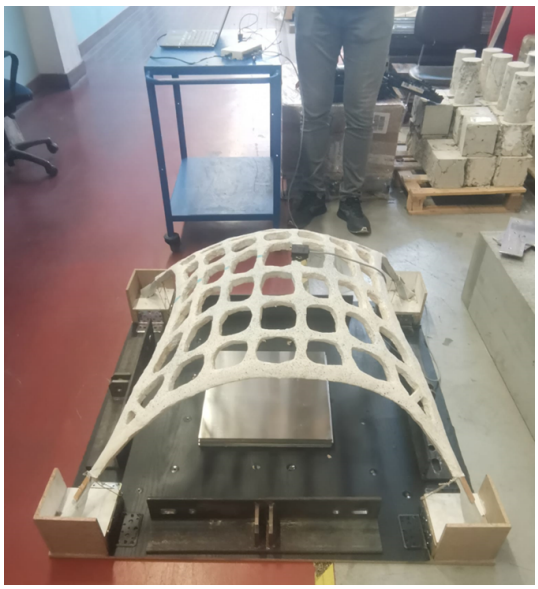

Fig. 3. Plywood base loaded with steel elements.

the same reference system. To provide a tight connection between the sensors and the structure, cable ties and double-sided adhesive tape were used to fix the sensor at the top, while screws firmly secure the other accelerometer.

3.3 Test and experimental methodology

Forced vibration testing refers to those techniques where the vibration is artificially induced, even if the excitation is not measured. The method can generally

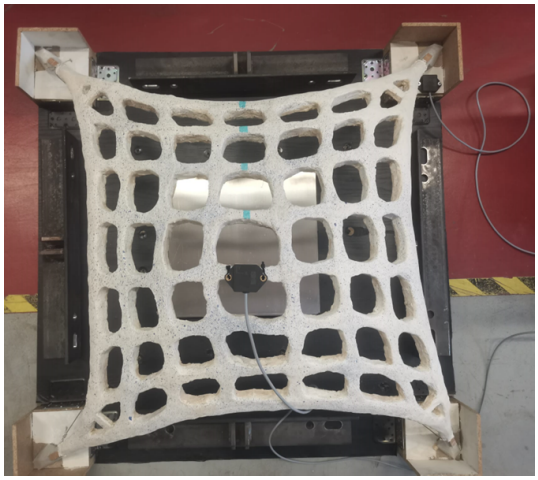

Fig. 4. Sensors layout.

be classed as transient testing if the input force is not measured. This mean of forced excitation can be divided into impulse testing, used herein, and step relaxation [22]. The simplest means of delivering an impact to a structure is by using a dropped weight or a hammer. Two different types of dynamic tests were performed: the first one has been performed by exciting the structure with a steel marble dropped on five different structure's points (the top of the grid shell and the keystone of the transverse arches), while the other one has been carried out hammering the same five points. The experimental test consisted of ten acquisitions of about 30 seconds, using a sampling rate of 200Hz.
Specifically, in order to investigate the response of the vault to different directions of the excitation source, the impact has been provided in $\pm X$, $\pm Y$ and $\pm Z$ axis corresponding to excitations along the two sides of the vault and the third one from the top to the bottom.

3.4 Results

In this section, the results obtained by the test performed with the hammer will be shown for clarity purposes. Additionality, the previous choice is justified by the significance of the results obtained during the acquisition phase. Due to the low weight of the steel marble, the resulting excitations on the structure were negligible and, consequentially, the accelerometer experienced difficulties in detecting the induced acceleration. For all these reasons, the authors decided to consider the acquisitions obtained by hammering the vault in five different positions.
Moreover, It has been recognized that the accelerations in the positive and negative sense of each axis show similar structural responses and comparable natural frequencies. Hence, the authors selected only the data obtained by hitting the

vault according to the positive sense of the X and Y axis and in the negative sense along the Z axis.
As depicted in Fig.s 5 (a)-(c)-(e), only the free vibration of the signal has been used for processing the FFT functions. For each direction, three curves have been plotted according to the output provided at the top of the vault, at the single support and the level of the shaking table.
The recorded data were processed through a Fast Fourier Transform (FFT) function to identify the fundamental frequencies of the structure.
By observing Figs. 5 (b)-(d), frequency domain outcomes highlight the first natural vibration frequencies with specific regard to the X and Y axis, respectively. For the accelerations along both X and Y, the peaks of the curves are observed for a value of the frequency equal to $15,77$ Hz. As expected, due to the symmetry of the structure, the transversal natural frequencies along x and y axes assume about the same values. On the contrary, focusing on the FFT along the Z axis, which is the direction in which the structure is obviously most rigid, a clearly-defined peak of the function has not been recognized within the observed frequency range. This is also consistent with preliminary observations conducted with FEM modelling, despite the uncertainties on the parameters, where the first frequency in the transverse direction settled at about $210,71$ Hz.

4 Comparison between numerical and experimental results

In this section, preliminary comparisons between the principal vibration modes obtained by the numerical model introduced in a previous work [23] and those derived by the experimental test will be shown. As reported in Table 2, a difference has been detected with regard to the natural frequency for the translation mode along X and Y directions, which represent the first and second vibration modes of the structure. More in detail, along the X and Y axis, corresponding to the first and second vibration modes respectively, the percentage variation between experimental and numerical results is equal to 39.5 and 46.2.
The inconsistency of these results could be addressed by the application of the mortar on the extrados and intrados sides of the bricks and, mainly, on the contact interface between two subsequent blocks. The intrinsic softness between the bricks could represent the main cause of the observed discrepancy. Due to the high frequency related to the translation mode along Z axis, no comparisons have been provided.

5 Conclusions and future developments

In this work, preliminary comparisons between numerical models and experimental tests have been shown. Specifically, an impulse test has been performed by hammering the structure or by adopting a steel marble dropped. The output obtained during the acquisition stage allow to point out the natural frequency of the translation modes along the X and Y axis. As expected, the vault

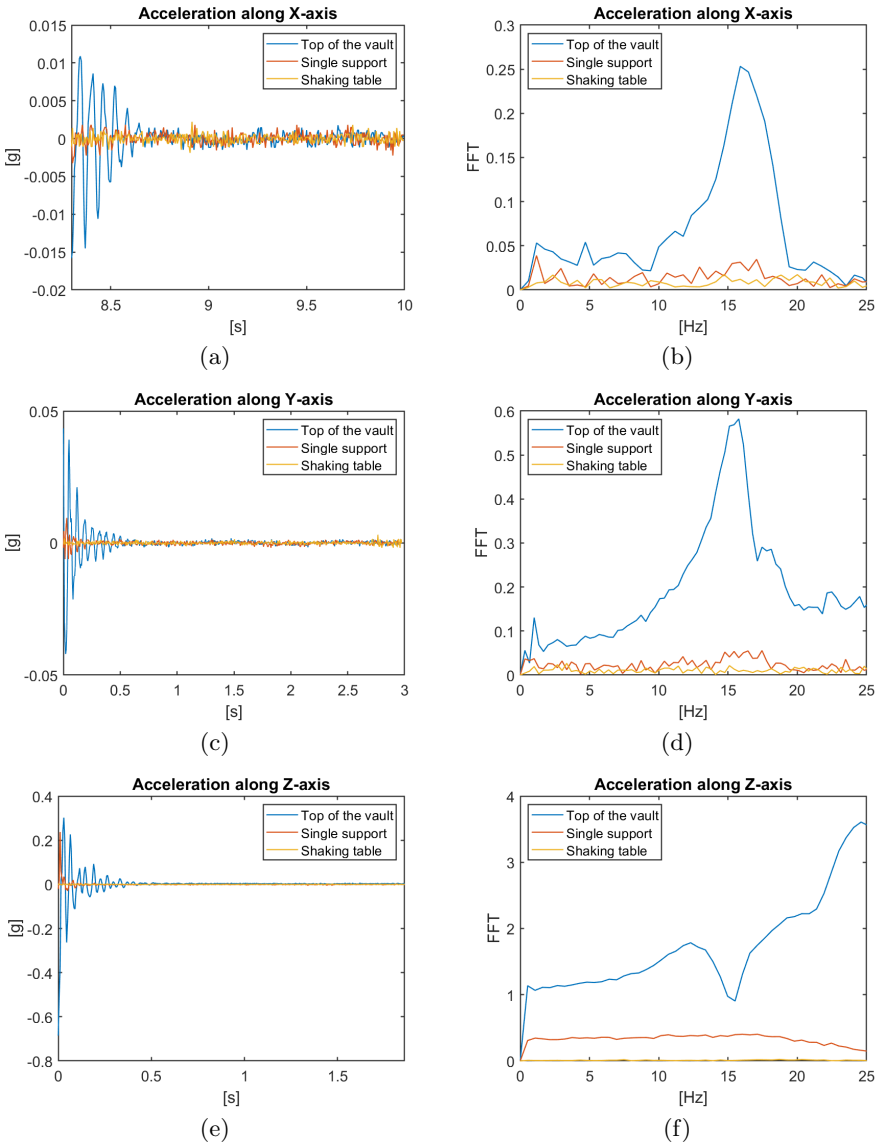

Fig. 5. Input acceleration (Fig.s (a)-(c)-(e)) and corresponding FFT functions (Fig.s (b)-(d)-(f)) along X, Y and Z axis, respectively

exhibits similar transversal vibration mode frequencies. Unfortunately, the frequency range representative of the vertical mode has been not recognized since the law frequency samples set during the test. By performing an eigenvalue analysis with the numerical model, already introduced in [23], the natural vibration mode along the Z axis has been detected around a frequency value equal to

Table 2. Comparisons between experimental and numerical results

Mode	**Numerical**	**Experimental**	
	Frequency $[Hz]$	Frequency $[Hz]$	Variation [%]
1	22.15	15.88	39.5
2	23.05	15.77	46.2
3	210.71		

210, 71 Hz. This fact is demonstrated by the trend of the FFT function in which a well-defined peak of frequency has been not detected.
However, it seems clear that the discrepancy in terms of percentage variation between experimental and numerical results can be addressed by the modelling strategies adopted during the model realization. It does not take into account the contribution of the mortar applied to the extrados and intrados surface of the vault which leads to a softness behaviour.
In future works, the validation of the numerical model will be provided by adopting a homogenized section of each element composing the structure. In this way, the contribution of the mortar will be considered in the global behaviour of the structure. Moreover, the effect related to slip phenomena and the role of the bond's condition between mortar and concrete should be investigated.
Finally, dynamic tests will be realized by using a suitable shaking table and the structural response over time will be discussed.

References

1. RIPPMANN, Matthias; LACHAUER, Lorenz; BLOCK, Philippe. Interactive vault design. International Journal of Space Structures, 2012, 27.4: 219-230.
2. OXMAN, Rivka; OXMAN, Robert. New structuralism: design, engineering and architectural technologies. Architectural Design, 2010, 4.80: 14-23.
3. MARANO, Giuseppe Carlo; TRENTADUE, Francesco; GRECO, Rita. Optimum design criteria for elastic structures subject to random dynamic loads. Engineering Optimization, 2006, 38.7: 853-871.
4. MARANO, Giuseppe Carlo; TRENTADUE, Francesco; PETRONE, Floriana. Optimal arch shape solution under static vertical loads. Acta Mechanica, 2014, 225.3: 679-686.
5. ROSSO, Marco Martino, et al. Enhanced multi-strategy particle swarm optimization for constrained problems with an evolutionary-strategies-based unfeasible local search operator. Applied Sciences, 2022, 12.5: 2285.
6. CUCUZZA, Raffaele; ROSSO, Marco Martino; MARANO, Giuseppe Carlo. Optimal preliminary design of variable section beams criterion. SN Applied Sciences, 2021, 3.8: 745.
7. CUCUZZA, Raffaele, et al. Optimal strengthening by steel truss arches in prestressed girder bridges. In: Proceedings of the Institution of Civil Engineers-Bridge Engineering. Thomas Telford Ltd, 2021. p. 1-21.

8. ROSSO, Marco Martino, et al. Structural Optimization With the Multistrategy PSO-ES Unfeasible Local Search Operator. In: Proceedings of International Conference on Data Science and Applications: ICDSA 2022, Volume 1. Singapore: Springer Nature Singapore, 2023. p. 215-229.
9. MELCHIORRE, Jonathan; BERTETTO, Amedeo Manuello; MARANO, Giuseppe Carlo. Application of a machine learning algorithm for the structural optimization of circular arches with different cross-sections. Journal of Applied Mathematics and Physics, 2021, 9.5: 1159-1170.
10. CUCUZZA, Raffaele, et al. Size and shape optimization of a guyed mast structure under wind, ice and seismic loading. Applied Sciences, 2022, 12.10: 4875.
11. ROSSO, Marco M., et al. Nonpenalty machine learning constraint handling using PSO-SVM for structural optimization. Advances in Civil Engineering, 2021, 2021: 1-17.
12. KILIAN, Axel. Design exploration through bidirectional modeling of constraints. 2006. PhD Thesis. Massachusetts Institute of Technology, Department of Architecture.
13. MANUELLO, A. Semi-rigid connection in timber structure: Stiffness reduction and instability interaction. International Journal of Structural Stability and Dynamics, 2020, 20.07: 2050072.
14. PEDERSEN, Pauli. Optimal joint positions for space trusses. Journal of the Structural Division, 1973, 99.12: 2459-2476.
15. RASMUSSEN, M. H.; STOLPE, Mathias. Global optimization of discrete truss topology design problems using a parallel cut-and-branch method. Computers & Structures, 2008, 86.13-14: 1527-1538.
16. TOĞAN, Vedat; DALOĞLU, Ayşe T. Optimization of 3d trusses with adaptive approach in genetic algorithms. Engineering Structures, 2006, 28.7: 1019-1027.
17. POST, Daniel. Moiré interferometry at VPI & SU. Experimental Mechanics, 1983, 23: 203-210.
18. De Mari, G., Domaneschi, M., Ismail, M., Martinelli, L. & Rodellar, J. Reduced-order coupled bidirectional modeling of the Roll-N-Cage isolator with application to the updated bridge benchmark. *Acta Mechanica*. **226** pp. 3533-3553 (2015)
19. Cimellaro, G. & Domaneschi, M. Stability analysis of different types of steel scaffolds. *Engineering Structures*. **152** pp. 535-548 (2017)
20. Domaneschi, M., Sigurdardottir, D. & Glisic, B. Damage detection on output-only monitoring of dynamic curvature in composite decks. *Structural Monitoring And Maintenance*. **4**, 1-15 (2017)
21. Tarantini, R., Cardoni, A., Marasco, S., Merlin, J., Pribaz, E., Rupolo, G., ... & Cimellaro, G. P. (2022, September). Dynamic Characterisation and Seismic Vulnerability Assessment of Existing Masonry Port Structures. In World Conference on Seismic Isolation (pp. 1032-1042). Cham: Springer International Publishing.
22. Salawu, O. S., & Williams, C. (1995). Review of full-scale dynamic testing of bridge structures. Engineering Structures, 17(2), 113–121. https://doi.org/10.1016/0141-0296(95)92642-l
23. Cucuzza, R., Cardoni, A., Manuello, A., Domaneschi, M., Cimellaro, G. P., & Marano, G. C. (2022). Experimental Investigation of the Static and Dynamic behaviors of 3D-Printed Shell Structures. WCCM-APCOM 2022, 900.